Fernández-Busnadiego et al., http://www.jcb.org/cgi/content/full/jcb.201206063/DC1

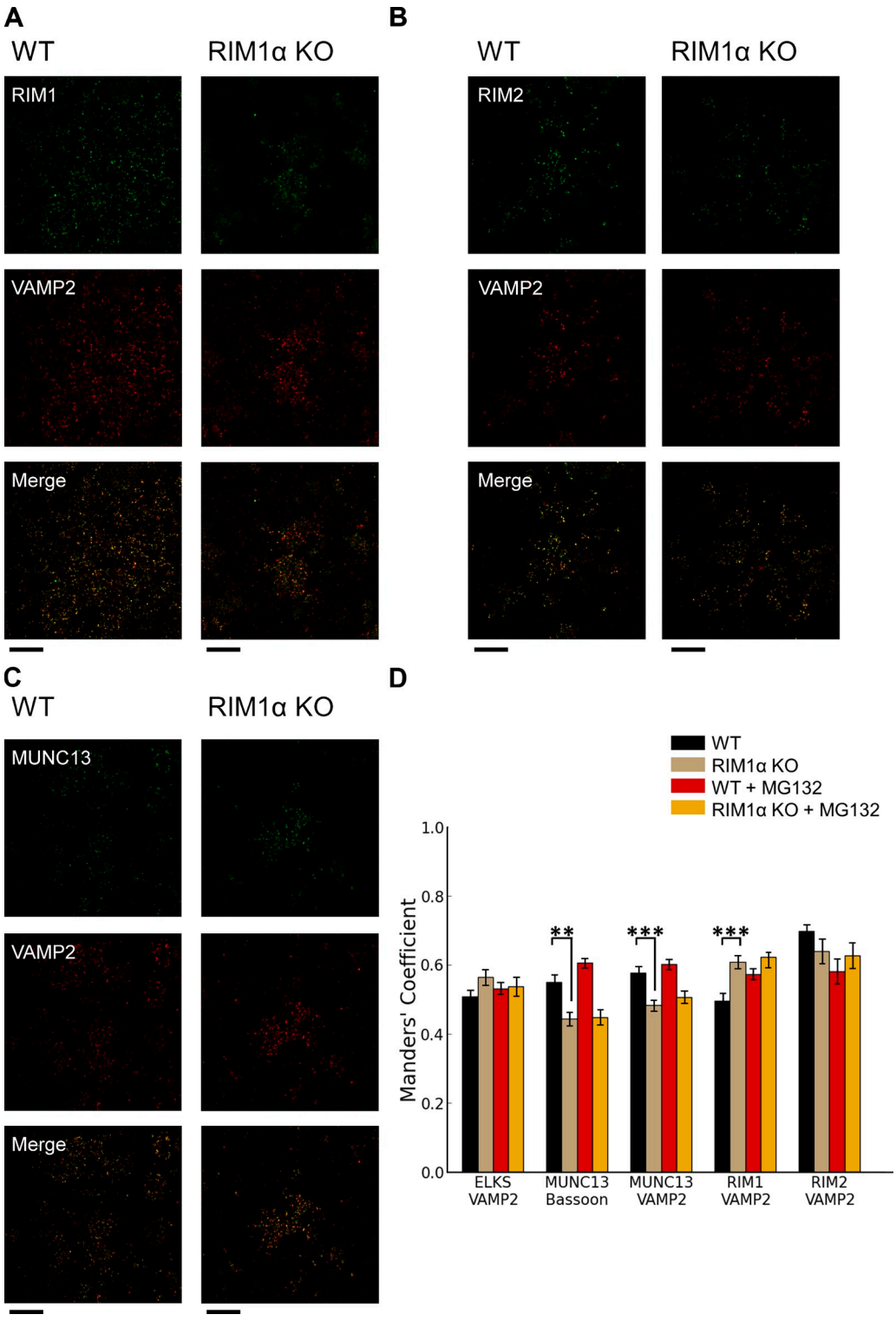

Figure S1. **Immunostaining for AZ proteins.** (A–C) Synaptosomes immobilized on coverslips were immunostained for VAMP2 (red) or Bassoon as presynaptic markers and for AZ proteins (green) including RIM1 (A), RIM2 (B), and MUNC13 (C). (D) Quantification of the fraction of AZ protein staining (ELKS, MUNC13, RIM1, and RIM2) colocalizing with presynaptic marker staining (VAMP2 and Bassoon), as measured by thresholded Manders' coefficients. Plot shows mean values and SEMs (error bars). Confidence values: **, $P < 0.01$; ***, $P < 0.001$ ($n = 5$ WT/ RIM1α KO littermate pairs, 15–20 images per condition). Bars, 20 µm.

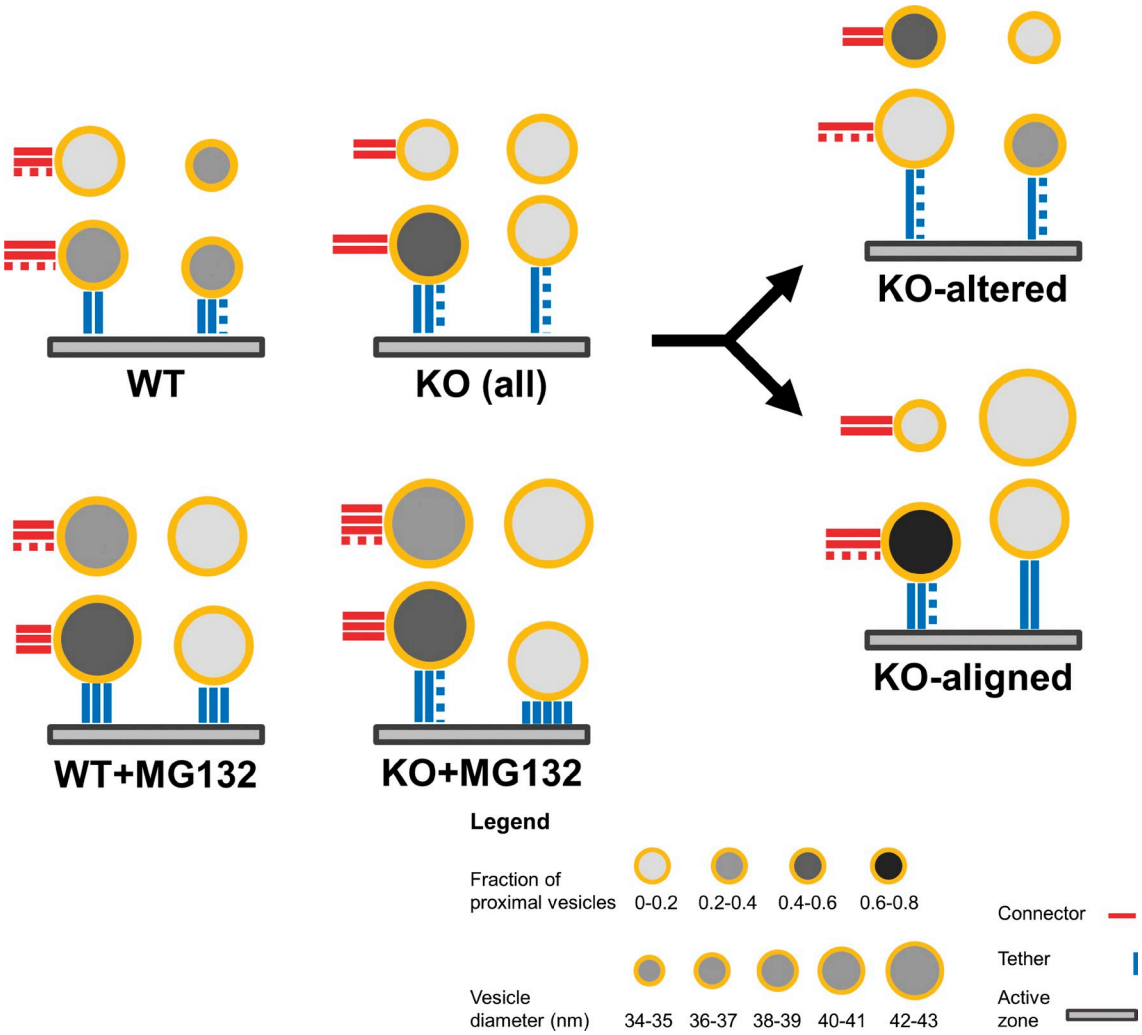

Figure S2. **Semiquantitative summary of tethering, connectivity, and vesicle diameter data for proximal vesicles (within 45 nm from the AZ).** For each group of samples, four circles represent vesicles tethered and connected (bottom left), tethered and not connected (bottom right), not tethered and connected (top left), and not tethered and not connected (top right). The fraction of total proximal vesicles represented by each class is shown by the grayscale value of the lumen (see legend). The diameter of the circle represents vesicle size (see legend). The lines emanating from vesicles represent connectors (red) and tethers (blue). Dotted lines represent half connector or tether. Connector and tether length are drawn to a different scale than vesicle size for visual purposes. The AZ is shown as a horizontal gray line.

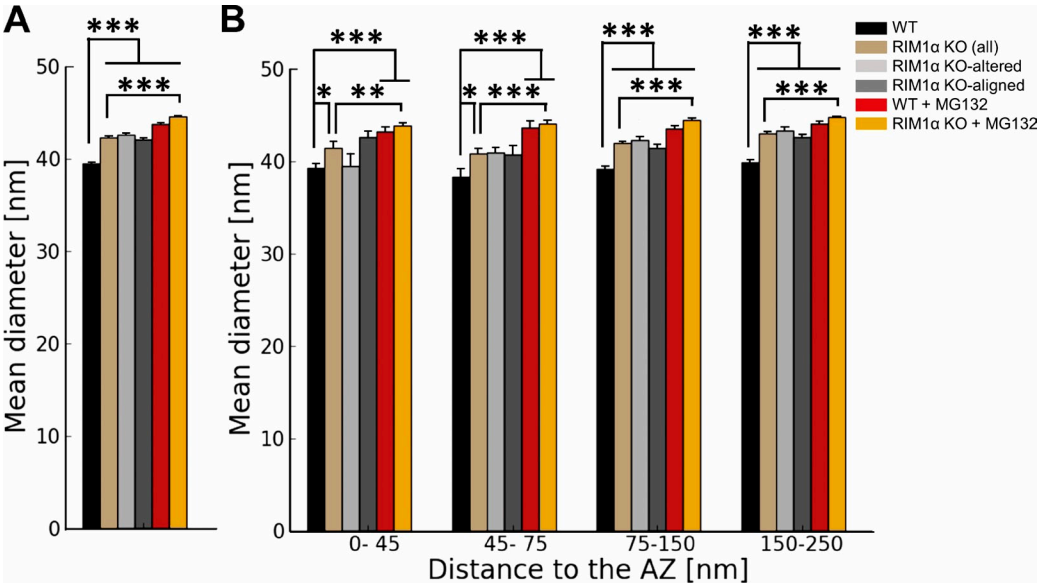

Figure S3. **Synaptic vesicle diameter for vesicles within 250 nm from the AZ.** Vesicle diameter increased in RIM1α KO and both in WT and RIM1α KO under MG132 treatment. (A) Mean vesicle diameter. (B) Vesicle diameter versus distance to the AZ. Plots show mean values and SEMs (error bars). Confidence values: *, P < 0.05; **, P < 0.01; ***, P < 0.001. The numbers of animals, synapses, and vesicles analyzed for each category are shown in Table S1.

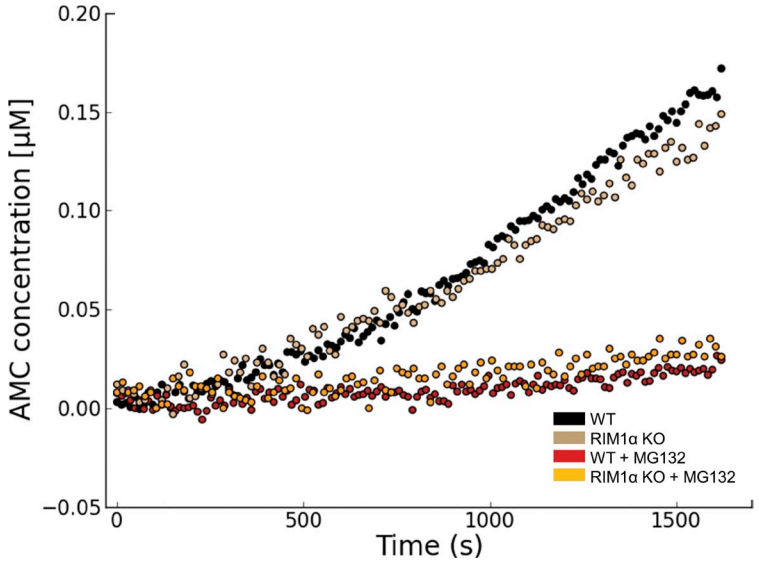

Figure S4. **Proteasome chymotryptic-like activity in synaptosomes (representative traces), measured as AMC fluorescence resulting from substrate (Suc-LLVY-AMC) degradation.** Proteasome activity was largely suppressed by MG132 treatment in both WT and RIM1α KO (*n* = 3 WT/ RIM1α KO littermate pairs).

Table S1. **Sample size for cryo-ET analysis**

Sample	Number of animals	Number of synapses	Total number of vesicles	Total number of tethers	Total number of connectors
WT	2	9	781	134	540
KO altered	3	4	494	11	673
KO aligned	3	5	450	60	1,079
KO (all)	3	9	944	71	1,752
WT + MG132	3	8	835	135	1,887
KO + MG132	2	14	1,681	160	5, 662
Total	8	49	5,185	571	11,593

Number of animals, synapses, synaptic vesicles, tethers, and connectors analyzed by cryo-ET for each category.

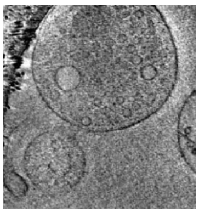

Video 1. **WT synapse.** Related to Fig. 1 (A and B). Cryo-ET of a cerebrocortical synaptosome from a WT mouse. Tilt series was collected from −64 to 54° with 2° angular increment in an electron microscope (Polara) using Xplore3D (FEI), reconstructed using TOM and rendered three-dimensionally using Amira. Tomograms were reconstructed using exact-weighted back projection to enhance visualization. Connectors and tethers were automatically detected using a Python package. First, tomographic slices along the z axis of the volume are shown. Then, renderings initially show all vesicles analyzed (within 250 nm from the AZ) and later proximal vesicles (within 45 nm from the AZ) only. AZ (gray), synaptic vesicles (yellow), tethers (blue), and connectors (red) are shown. For scale reference, mean vesicle diameter was 40.1 ± 5.4 nm (mean ± SD; no scale bars are shown because the image is rendered with 3D perspective). Note that the WT synapse contains numerous proximal vesicles and that most of them are tethered to the AZ.

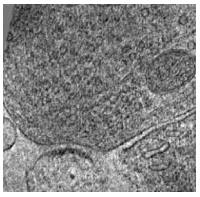

Video 2. **KO-altered synapse.** Related to Fig. 1 (D and E). Cryo-ET of a cerebrocortical synaptosome from a RIM1α KO mouse. Tilt series was collected from −60 to 60° with 2° angular increment in an electron microscope (Polara) using Xplore3D (FEI), reconstructed using TOM, and rendered three-dimensionally using Amira. Tomograms were reconstructed using exact-weighted back projection to enhance visualization. Connectors and tethers were automatically detected using a Python package. First, tomographic slices along the z axis of the volume are shown. Then, renderings initially show all vesicles analyzed (within 250 nm from the AZ) and later proximal vesicles (within 45 nm from the AZ) only. AZ (gray), synaptic vesicles (yellow), tethers (blue), and connectors (red) are shown. For scale reference, mean vesicle diameter was 40.1 ± 5.4 nm (mean ± SD; no scale bars are shown because the image is rendered with 3D perspective). Note that, in comparison to WT, the RIM1α KO-altered synapse contains less proximal vesicles and few of them are tethered to the AZ.

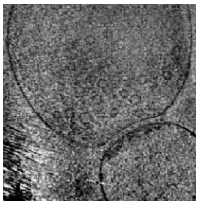

Video 3. **KO-aligned synapse.** Related to Fig. 1 (F and G). Cryo-ET of a cerebrocortical synaptosome from a RIM1α KO mouse. Tilt series was collected from −54 to 54° with 2° angular increment in an electron microscope (Polara) using Xplore3D (FEI), reconstructed using TOM, and rendered three-dimensionally using Amira. Tomograms were reconstructed using exact-weighted back projection to enhance visualization. Connectors and tethers were automatically detected using a Python package. First, tomographic slices along the z axis of the volume are shown. Then, renderings initially show all vesicles analyzed (within 250 nm from the AZ) and later proximal vesicles (within 45 nm from the AZ) only. AZ (gray), synaptic vesicles (yellow), tethers (blue), and connectors (red) are shown. For scale reference, mean vesicle diameter was 40.1 ± 5.4 nm (mean ± SD; no scale bars are shown because the image is rendered with 3D perspective). Note that, in comparison to WT, the KO-aligned synapse contains a similar number of proximal vesicles and similar degree of tethering to the AZ.

Supplemental material also includes a ZIP file that contains a code that was used to perform statistical analysis of the segmentation results and plot all graphs shown in this paper.